

Saturation and voltage quenching of porous-silicon luminescence and the importance of the Auger effect

I. Mihalcescu, J. C. Vial, A. Bsiesy, F. Muller, and R. Romestain

Laboratoire de Spectrométrie Physique, Université Joseph Fourier and CNRS, Boîte Postale 53X, 38041 Grenoble Cedex, France

E. Martin, C. Delerue, M. Lannoo, and G. Allan

Institut d'Electronique et de Microélectronique du Nord, Département Institut Supérieur d'Electronique du Nord, 41 boulevard Vauban, 59046 Lille Cédex, France

(Received 30 September 1994)

Two important observations for porous silicon, the saturation and the voltage selective quenching of photoluminescence, are presented. Their similarities are pointed out and discussed in two phenomenological models: the saturation of the absorption and an Auger effect. The consequences of carrier accumulation in quantum crystallites are emphasized in both cases. The rate of Auger recombination in quantum crystallites is calculated theoretically and is compared to experiments. The importance of the Auger effect is then checked in the mechanisms of the voltage tunable electroluminescence.

I. INTRODUCTION

Since the first experimental results concerning intense visible photoluminescence (PL) obtained on highly porous silicon layers were published,¹ a great deal of work has been devoted to the understanding of this property. Different physical origins have been proposed. Among these hypotheses, the quantum confinement of free carriers, taking place inside the interconnected silicon nanocrystallites^{1,2} forming the body of the highly porous silicon layers, seems at present to be most supported.

The quantum confinement model has been extended for a description of the nonradiative processes³ (W_{nr}), and to explain the efficient electroluminescence (EL) obtained when carriers are supplied by an electrolyte and by the silicon substrate under polarization.⁴ The aim of this paper is to show that effects consisting of a selective voltage PL quenching⁵ as well as the observation of a PL intensity saturation can be seen as illustrations of the carrier accumulation in quantum crystallites leading to a reduction of the absorption coefficient or a strong enhancement of the nonradiative recombination rates. Simple phenomenological models are suggested for both hypotheses, and an Auger process is proposed for a quantitative explanation. This idea is then extended to a revisitation of the voltage tunable electroluminescence phenomenon.

II. EXPERIMENT

A. Experimental procedures

In this paper we will describe mainly two types of experiments: the voltage quenching of PL (VQPL) and the saturation of PL (SPL). For VQPL experiments porous silicon is obtained by electrochemical etching of lightly doped *n*-type ($8 \cdot 10^{14}/\text{cm}^3$) substrates. The electrolyte is a 3:5:2, hydrofluoric acid (HF)-(49wt%):ethanol:deionized water mixture. The front side of the sample is illuminat-

ed by a tungsten lamp ($40 \text{ mW}/\text{cm}^2$) in order to provide the hole concentration necessary for a nanoporous-type layer formation. With this procedure, homogeneous layers were obtained for thicknesses up to $1 \mu\text{m}$. Immediately after anodization, the HF electrolyte is evacuated, and the sample rinsed in deionized water and then put into a $1M$ aqueous solution of sulfuric acid. A negative-potential scan was then applied vs a reference standard calomel electrode (SCE) at $25 \text{ mV}/\text{s}$. The continuous-wave-excited PL obtained under an excitation of a 458-nm line of an argon laser is then recorded using an optical multichannel analyzer.

For SPL experiments different lightly doped *p*-type samples with different porosities (from 65% to 80%), as-formed or anodically oxidized, fresh or two years old, with thicknesses varying from 0.1 to $40 \mu\text{m}$ were used. In order to avoid thermal effects, we used N_2 laser excitation (excitation well above the band gap: $\lambda = 337 \text{ nm}$) with a pulse width of 3 ns and a repetition rate of 20 Hz . The temporal resolution of the analysis chain was about 5 ns . The laser beam was unfocused (area $\approx 0.7 \text{ cm}^2$) or slightly focused (area $\approx 0.2 \text{ cm}^2$) when higher excitation densities were required. The maximum beam energy was of about $125 \mu\text{J}/\text{pulse}$, and we changed it using a set of calibrated attenuators. All measurements were made at room temperature.

Figure 1 shows a typical time evolution of the PL which follows a short pulse excitation. This particular plot clearly shows two components which have independent dependences against various parameters:⁶ a fast component with a lifetime less than 20 ns and a much slower component. The PL intensities of these two components are defined by their respective areas under the PL time evolution curve (see Fig. 1). A shape analysis of the fast component is beyond our experimental possibilities. Concerning the slow component, its decay versus time $f(t)$ is not exponential, but quantitative analysis can be performed through the mean lifetime:

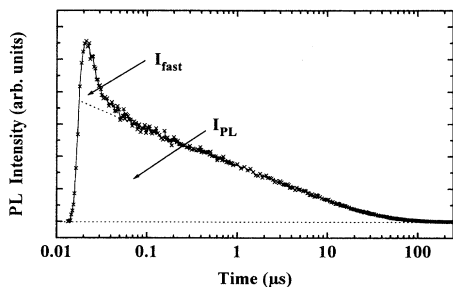


FIG. 1. A typical PL (detected at 700 nm) time evolution following short pulse excitation. The unusual log time axis has been used to emphasize the two different components.

$$\tau = \frac{1}{f(0)} \int f(t) dt,$$

where $f(0)$ is the intensity just after the pulsed excitation (practically 100 ns after the pulse excitation in order to cancel the effect of the fast component).

Mean lifetime measurements provide a powerful tool for the study of the mechanisms at the origin of visible light emission from porous silicon.³ The mean lifetimes are long (for good samples at room temperature in the range of μ s to ms) and show a high sensitivity to parameters as different as the level of passivation or the temperature, for example. It has been shown that this sensitivity, at room temperature and above, is mainly due to the variation of the nonradiative processes. However, as sensitive as this technique can be, it is limited by the time resolution of our experimental setup. That is to say that very efficient quenching processes giving rise to lifetimes shorter than this time resolution will not be seen in the time domain.

For the SPL experiments, it is important to control the amount of light absorbed. This is usually performed by a transmission measurement, but cannot be used here because the porous layers are attached to the opaque silicon substrate. We have discovered that a simple photoacoustic⁷ technique is convenient for this purpose. A typical audible photoacoustic signal detected by a commercial microphone (bandwidth 20 kHz) is shown in Fig. 2. The

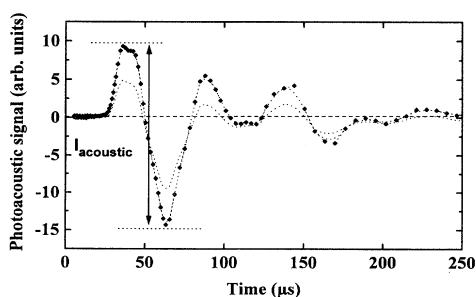


FIG. 2. Typical photoacoustic signals generated by short pulse excitation of a 65% porosity layer in ambient air. The two curves, obtained with two different excitation powers, have the same shape, and have amplitudes proportional to the excitation intensity.

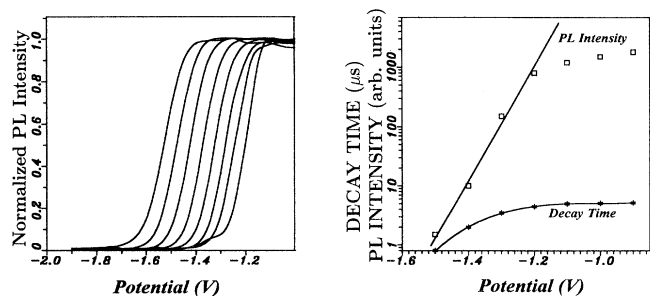


FIG. 3. Left part: PL intensity as a function of the applied voltage (referred to the saturated calomel electrode) for various luminescence energies (from left to right: 2, 1.88, 1.77, 1.68, 1.59, 1.51, 1.44, and 1.35 eV). Right part: Simultaneous measurement of the PL intensity and decay time recorded at 700 nm as a function of the cathodic potential. The fit of the intensity corresponds to the law $I_{PL} \propto \exp(-eV/s)$ with $s = 40$ meV. For the lower curve, the continuous line is just a guide for the eyes.

temporal evolution cannot be used for physical information because of the limited bandwidth of the microphone, but its peak-to-peak amplitude is directly proportional to the absorbed light. In addition, we have verified that the photoacoustic technique is very well suited for the study of the porous material: the signal is emitted by the porous layer and not from the substrate.

The fast PL component can also be used to monitor the porous layer absorption. The blue luminescence is probably due to a kind of color center⁶ located in the Si oxide interface. Its excitation is in fact a good probe for the light absorption.

B. Experimental results

1. Voltage selective quenching of the PL

An analysis of the voltage tunable EL and the voltage selective quenching of the PL has already been done;⁸ it has pointed out the importance of the selective injection of carriers. Figure 3 shows the very efficient voltage selective quenching compared with the relative stability of the mean lifetime. An important observation is the voltage selectivity shown in the left part of Fig. 3. The various curves of the PL intensity versus the applied voltage are well fitted⁸ by carrier statistical laws, which indicates that the carrier injection is at the origin of the quenching.

An analysis of how the carrier injection can affect the PL efficiency has already been done in Ref. 8, and here we will just recall the hypothesis, which can also be used for the analysis of the saturation effect discussed in Sec. III B 2. A possible explanation could be the decrease of the number of optically active sources as a result of the electron accumulation (driven by the cathodic bias) into the Si nanocrystallites, which can make these entities transparent to the excitation wavelength. If we consider a Si nanocrystallite without an external bias, the confined electronic levels are unoccupied and excitation absorption is possible, giving rise to the observed orange-red

PL. Once the electronic levels are occupied due to the electron flow coming from the substrate, it is no longer possible to photogenerate an electron-hole pair, the excitation is no longer absorbed, and this crystallite becomes optically inactive. Another possibility is a strong enhancement of the nonradiative processes which can have two origins: (i) An increase of the nonthermalized carrier escape probability across the energy barriers surrounding the Si nanocrystallites; this barrier modification being induced by the cathodic polarization. (ii) An Auger process taking place as soon as a carrier is added (by electrical injection) to an electron-hole pair photogenerated in a crystallite.

2. The PL saturation

Evidence of the intensity saturation of PL is given in Fig. 4, where the luminescence intensity varies linearly for low intensity excitation and saturates at higher flux. In this figure the other important information is the stability of the mean lifetime under the same excitation variation. Similar curves are also observed for very thick samples such as a 10- μm 65% anodic oxidized sample or a 40- μm self-supported one. The intensity saturation of the PL of porous silicon has already been reported,⁹ but with cw excitation and without information on the decay times. Figure 5 provides information about the same excitation range: the photoacoustic signal and the fast component of the PL both have a linear dependence in the full range of the excitation. As previously pointed out, this indicates that light absorbed by the porous layer is still a linear function of the incident light intensity. Here we have to point out that the absorption linearity is only valid within our excitation range, in contrast to what has been obtained at much higher excitation power by picosecond laser excitation.¹⁰

III. DISCUSSION

A. Phenomenological description

There are many possible origins for the saturation and voltage quenching of the PL. We will focus here on common explanations justified by large similarities in the two phenomena. Sample heating is the first simple hypothesis to consider. It is well known that the PL decreases when

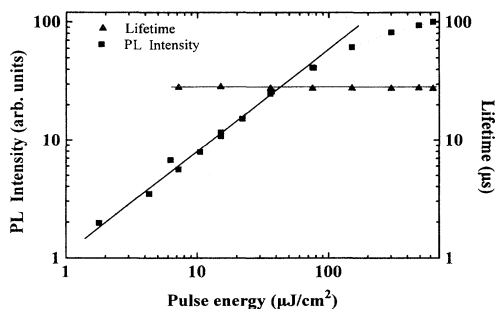


FIG. 4. Evolution of the PL intensity and average lifetime for a 700-nm wavelength as a function of the energy of pulse excitation (for 1- μm 65% anodic oxidized sample).

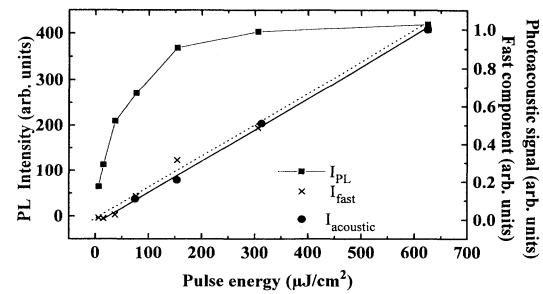


FIG. 5. Comparison of the PL intensity (for the slow and fast components) and the photoacoustic signal as a function of the excitation intensity for 1- μm 65% anodically oxidized sample.

the temperature increases above room temperature, but this is associated with a shortening of the lifetimes.³ A shortening of the lifetime has not been observed during the quenching or saturation, so this explanation can be excluded except if, for the saturation effect, the heating and cooling cycle is short enough to occur during the excitation pulse. This can happen when the thin porous-silicon layer is in contact with the bulk substrate, which acts as a heat sink. As previously pointed out the same saturation effect has been observed for very thick and free-standing layers, so this hypothesis can be eliminated definitively. In addition, considering the simple and limiting case where all the excitation energy is transformed into heat during a $\approx 125\text{-}\mu\text{J}$ short pulse focused on 0.20- cm^2 surface of a 1- μm -thick porous layer (of 80% porosity), a simple calculation gives a temperature increase of $\Delta T = 15$ K. This is not sufficient to induce a noticeable quenching of the PL. Finally, a temperature increase is known to induce a redshift of the porous layer emission. Conversely, as shown in Fig. 6, the PL saturates along with a blueshift (this fact has already been pointed out in Ref. 9).

We propose two other possible mechanisms for the PL saturation and PL quenching: (i) a selective saturation of the absorption which affects the luminescence part of the porous silicon, and (ii) an Auger effect which strongly increases the nonradiative recombination rates. In the two cases we will adopt, as a first step, a phenomenological approach for an analysis of their consequences.

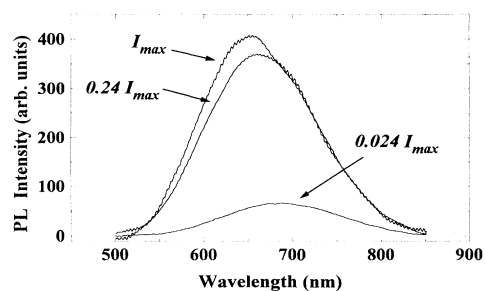


FIG. 6. PL spectral dependence on the excitation intensity for an anodically oxidized porous layer of 65% porosity and 1- μm thickness.

1. The selective absorption saturation

Porous silicon is an inhomogeneous material. A maximum of 5% of its PL quantum efficiency obtained for very good samples indicates that a large proportion of the material is nonluminescent. So we will idealize the material by considering only two phases: the luminescent (L) and nonluminescent (NL). We will suppose in addition that the absorption of the L centers, hidden by the NL centers, is the only one to saturate at moderate flux, and this is the meaning of the expression "selective absorption saturation." Briefly, this description follows the idea of a material made up of a distribution of a small quantity of well-passivated crystallites (with small W_{nr}) embedded in a large amount of badly passivated crystallites (with large W_{nr}).

Detailed analyses of the luminescence dynamics at high and low temperatures^{3,11} have shown that the L centers have high absorption cross sections in the UV and metastable states in the visible, with luminescence lifetimes in the range of 10–100 μ s. An efficient population storage can then be expected, leading to a noticeable depopulation of the ground state when the excitation is provided by short pulses. Figure 7 shows the optical cycle for L centers with a strong transition $0 \rightarrow 1^*$ followed by a fast relaxation to the metastable state 1. The following rate equations describe this optical cycle:

$$dN_0/dt = -N_0\sigma i \quad \text{and} \quad N_1 + N_0 = N,$$

where N is the total concentration of optical centers, i the flux of photons, and σ the cross section for the transition $0 \rightarrow 1^*$. Therefore at the end of the excitation pulse, the number of incident photons (per unit surface) being I , the solution of this equation gives a ground-state population proportional to $\exp(-\sigma I)$, and consequently the luminescence intensity I_{PL} is

$$I_{PL} \propto 1 - \exp(-\sigma I). \quad (1)$$

In fact this expression is valid in the small absorption condition; for samples of thickness l the attenuation of I (due to the absorption by the NL centers) has to be taken into account so the intensity of luminescence I_{PL} becomes

$$I_{PL} \propto \int_0^l \{1 - \exp(-\sigma I_0 \exp[-\alpha x])\} dx, \quad (2)$$

where α is the absorption coefficient of the porous layer.

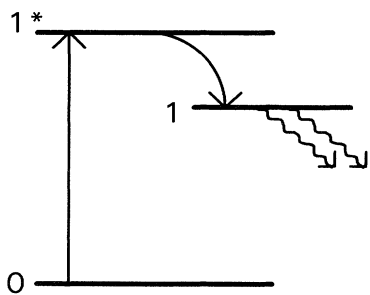


FIG. 7. Simple energy diagram showing the absorption from ground state to an excited state followed by a fast relaxation to the luminescent metastable state.

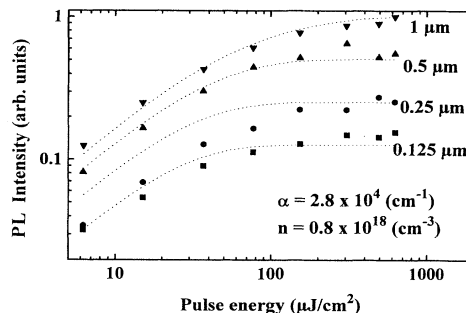


FIG. 8. Saturation of the PL for four samples of different thicknesses, and for the best fit following expression (2) with the parameters written inside.

Equation (2) can be used to fit the experimental data obtained for samples of 80% porosity and of various thicknesses. If we suppose that the L and NL centers have the same cross section σ , another useful parameter is the density of absorbing centers $n = \alpha/\sigma$.

Figure 8 shows the experimental results and their best fit using a realistic $3 \times 10^4 \text{ cm}^{-1}$ absorption coefficient¹² and an absorbing center concentration $n = 0.8 \times 10^{18} \text{ cm}^{-3}$. This result gives us confidence in our phenomenological approach; in addition, it provides a natural explanation for the stability of the lifetimes. Nevertheless, recall that our purpose was to find a common explanation for the PL saturation and PL quenching. The above model is only valid for the PL saturation, but it has the advantage of showing the following: Any model adapted to the quenching phenomenon which leads to an expression similar to expression (1) will be well suited. The Auger effect is an example which follows this rule, and we will develop this point now.

2. Phenomenological treatment of the Auger effect

The idea is quite simple: nonradiative rates can be strongly enhanced when more excitations than one are simultaneously present in a crystallite. The Auger effect belongs to this category, but other mechanisms can be found, such as the excitation transfer leading to the fusion of excitation, a common phenomenon in molecular physics.

Figure 9 shows an optical cycle for crystallites which

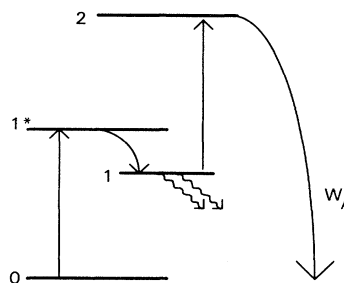


FIG. 9. Simple energy diagram showing the double excitation of a crystallite followed by an Auger relaxation, while the metastable state of the singly excited crystallite remains luminescent.

can be singly or doubly excited. The two-step excitation process can be generalized to more than two, but this is not necessary since the Auger process (with rate W_A) starts to be very efficient as soon as three carriers (an exciton plus a carrier belonging to another exciton, for example) interact. Figure 9 is drawn for the case of the creation of two excitons, but can easily be modified by one optically created exciton plus one electrically injected carrier, which is a scheme more representative of the voltage quenching of the PL.

During the optical cycle represented in Fig. 9, the population is shared between various states of the crystallites, while the light is mainly emitted by the singly excited crystallites (level 1) because the doubly excited state is quenched by the Auger effect. It is possible to write and solve the rate equation for this cycle, but it is simpler to remark that there is a great similarity to the case of the selective absorption saturation discussed earlier: indeed, doubly excited crystallites can be seen as nonluminescent (NL) crystallites; therefore an expression similar to expression (1) also represents the light emission in the case of an Auger quenching. It must be noted that in this model the light absorption which cumulates the first and second steps has still a linear dependence on the excitation intensity, even in the regime where the emission starts to saturate.

B. The physical basis of the absorption saturation and the Auger effect

In the experiments reported in this paper, an important result has been the high stability of the lifetimes along with the luminescence quenching and saturation. While the selective absorption saturation gives an obvious reason for that, it is not easy to understand why an increase in nonradiative processes (the Auger process) is accompanied by a reduction of the lifetimes as is the case for the Auger effect in bulk semiconductors.¹³ We believe that this is another illustration of the confinement effect. For bulk semiconductors the carriers are all equivalent, and an increase in carrier density has the same effect for all carriers. In our case, the statistics are different; the population of singly excited crystallites (with small W_{nr}) and the population of doubly excited crystallites (with high W_{nr}) both have to be considered, and the time evolution is the sum of the two contributions. We will see below that W_{nr} for doubly excited crystallites, is large enough to give very short decay time which cannot be resolved by our experimental setup. Consequently the decays are only representative of the singly excited crystallites, and a lifetime shortening is not expected. Conversely, the PL intensity is still strongly affected by the Auger effect.

1. Possible origins of the selective absorption saturation

The absorption saturation for three-level systems having a long-lived intermediate level has been very often encountered in systems as different as semiconductors,¹⁴ organic and inorganic insulators,¹⁵ and liquid dyes. Siloxene has been proposed as a chromophore naturally present in porous silicon. Without entering into the con-

troversy, its molecularlike nature, with an excited triplet state, makes it a possible candidate, but we will not follow this route since many other arguments have eliminated it.¹⁶

For semiconductors, the localization of carriers (or at best the trapped excitons on isoelectronic carriers) (Ref. 17) is the most favorable situation for the absorption saturation. It must be noted that intraband transitions have also shown this behavior, but at much higher excitation intensities.¹⁸ Taking into account these examples, we believe that the easy saturation effect (occurring at low excitation intensity) is another illustration of carrier localization in porous silicon. In that sense the model of Koch, Petrova-Koch, and Muschick,¹² where the excitation is trapped in surface states, is certainly a favorable situation for absorption saturation. But it is not the only situation: porous silicon seen as a distribution of interconnected quantum dots has shown its ability to efficiently localize the carriers. One can argue that, even with nanometric size, crystallites still have a large number of atoms which render the saturation as difficult as for the bulk. In fact crystallites are better described as quantum dots with finite barriers (a barrier height of 1 eV seems an upper limit for the electrons, as demonstrated by temperature measurements¹⁹), so there is a limited number of localized states in each crystallite. More precisely, taking into account the orbit valley degeneracy, only $p=6$ electron-hole pairs can fit in the ground state of a silicon quantum dot. It is then easy to take this fact into account by introducing, in the diagram of Fig. 7, a multilevel excitation. Expression (1) is then modified by changing σ in σ/p in it. Therefore the fit shown in Fig. 8 remains valid, but with parameters slightly modified.²⁰

2. Orders of magnitude for the Auger effect in porous silicon

While to our knowledge it is new to invoke an Auger process for electrical quenching of the photoluminescence, the Auger recombination has proved its efficiency many times, in situations similar to ours. The best examples are given for excitons trapped on neutral donors or acceptors in GaP (Ref. 21) and Si²², both indirect-band-gap semiconductors, or for free carriers in highly doped¹³ and lightly doped but highly excited²³ silicon, or for geminate electron-hole pairs in amorphous silicon.^{24,25} More recently Ghanassi *et al.*²⁶ have shown that efficient Auger effect can also occur in II-VI quantum dots.

The Auger effect is a three-carrier interaction where an electron-hole pair transfers its energy nonradiatively to a third nearby carrier. Therefore, for bulk semiconductors, the probability per unit time for an Auger reaction R is proportional to the product of carrier population concerned in the reaction. For n -type bulk silicon for example, R is

$$R \propto p(n+N)(n+N),$$

while for intrinsic semiconductors it is

$$R \propto Apn^2 + Bnp^2,$$

where p and n are the optically created electron-hole population (therefore $p=n$) and N the majority-carrier con-

centration. For highly doped semiconductors and in a small flux condition ($n \ll N$), R becomes simply $R \propto p \cdot N^2$. Consequently the rate equation for the minority carrier is

$$dp/dt = -AN^2p,$$

which gives an exponential decay and then allows the experimental determination of the Auger rate constant (A). Dziejwior and Schmid¹³ measured an Auger rate constant of $10^{-31} \text{ cm}^6 \text{ s}^{-1}$ while Yablonovitch and Gmitter,²³ in the intrinsic case, deduce a slightly higher value. These measurements can be used to estimate the Auger effect in our situation. The silicon quantum crystallites (occupied by an electron hole pair plus one or two carriers) with volume V in the order of 10^{-20} cm^3 can be seen as a silicon region where the density of carriers is $1/V$ therefore the Auger rate is expected to be $10^9 - 10^{10} \text{ s}^{-1}$, i.e., τ in the subnanosecond range. This Auger decay time is shorter than our experimental resolution and therefore can explain why we were not able to detect any modification of the decay time (as explained in Sec. III B 1) but just a reduction of the intensity, for the saturation measurements as well as for the voltage quenching experiment.

However, this estimation of the Auger decay time is *a priori* very crude since it assumes that the Auger rate constant is the same in silicon quantum crystallites as in bulk silicon. Therefore, we have performed a detailed calculation of the Auger recombination in such confined systems. Interestingly, we will see that the very simple estimation gives the correct order of magnitude for reasons we want to emphasize.

3. Detailed calculation of the Auger rate in silicon crystallites

There have been many attempts to calculate the Auger lifetime in bulk semiconductors.²⁷ We have made the calculation in the case of isolated spherical silicon crystallites whose surfaces are terminated by hydrogen atoms to avoid localized states.²⁸ As usual, the probability per unit time $W = 1/\tau$ is given by the Fermi rule²⁷

$$W = \frac{4\pi^2}{h} \sum_{i,f} p(i) |H_{i,f}|^2 \delta(E_f - E_i). \quad (3)$$

The initial states i correspond to the system with one electron-hole pair and a third carrier, $p(i)$ being their probability of occupation. In the final states f , the electron hole has recombined and transferred its energy to the third carrier. Assuming determinantal eigenfunctions for the initial and final states, this many-electron problem can be reduced to a calculation of matrix elements of the screened Coulomb potential $1/\epsilon r$ involving one-electron wave functions.²⁷ The summation in expression (3) is over all possible initial and final states with the constraint of energy conservation. The simplest case corresponds to the normal Auger process, i.e., without phonon assistance, where terms in expression (3) are purely electronic. In the case of bulk semiconductors, there are many nonvanishing terms following these requirements and one obtains complicated integration in the k space.²⁷ In the

case of a crystallite, the situation is completely different because the energy spectrum is made of discrete levels. For example, for a spherical crystallite of diameter 3.9 nm containing about 1500 silicon atoms, we have calculated²⁸ an average spacing between levels of about 10 meV even in energy regions with higher density of states. Because of the quantization, there is no way to fulfill the energy conservation rule, since it is impossible to excite the third carrier with an excitation energy exactly matching the electron-hole pair energy. In consequence, in the case of a crystallite, there is no purely electronic contribution to expression (3). To obtain nonvanishing terms, we need to take into account the various possible broadenings of the electronic levels. Of course, in the case of porous silicon the crystallites are not isolated; they are just separated by silicon bridges or silicon oxide barriers, for example. The broadening induced by these connections is probably substantial above all in the energy range far from the band gap, where the influence of the electronic states of the barriers is at a maximum. This will be discussed at the end of this section. Another origin for the broadening is the electron-phonon coupling. Recently,²⁹ we have shown that there is a strong lattice relaxation after the creation of an electron-hole pair in a crystallite, because it corresponds to the transfer of an electron from a bondinglike state (valence) to an antibondinglike state (conduction). In the case of the Auger process, the initial and final states also differ by one electron-hole pair, and a similar lattice relaxation must occur. The energy of the relaxation, the Franck-Condon shift, is between 3 and 15 meV depending on the size of the crystallite.²⁹ With such a strong coupling and in the high-temperature limit (300 K), the Dirac function in expression (3) is just replaced by a Gaussian whose width is fixed by the Franck-Condon shift.³⁰

The calculation is now straightforward. The matrix element in expression (3) is taken to be independent of the electron-phonon coupling. The electronic states are defined by Slater determinants built from one-electron wave functions. These latter are described in a basis of localized atomic states following the tight-binding calculation described in Ref. 29. The advantage of this technique is that the matrix elements of the screened Coulomb potential $1/\epsilon r$ are easily calculated in the basis of atomic wave functions²⁹ because electronic charges localized on atoms can be reasonably approximated by point charges. For the dielectric constant, we have used the bulk silicon value $\epsilon = 11.7$, except for intraatomic Coulomb terms which are evaluated using a q -dependent ϵ .²⁹ In expression (3), even at room temperature, only the initial state with the lowest energy is populated because of the large level splitting due to the strong confinement (for degenerate or nearly degenerate levels, an average Auger lifetime has been calculated). For final states, the remaining carrier is allowed to explore all the available levels.

Results for the calculated Auger lifetime are plotted in Figs. 10 and 11. The scattering of the results is quite large because the electron-hole energy can be more or less close to the possible excitation energies of the third carrier. The Auger recombination, most of the time, is faster than

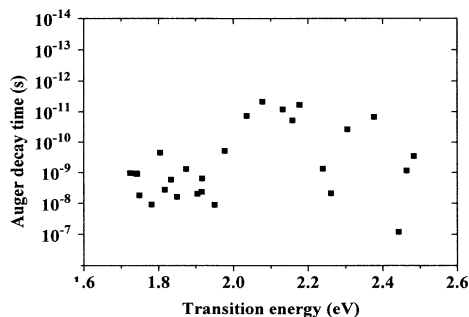


FIG. 10. Calculated lifetime for the Auger recombination in spherical silicon crystallites with respect to the calculated electronic gap. Here the Auger process involves two electrons and one hole.

10 ns, i.e., much faster than the calculated radiative lifetime.²⁸ The results are quite close to the crude estimate made from the bulk silicon Auger lifetime. We can explain this quite surprising result by the fact that the electron-phonon coupling is already sufficiently large to smooth the effect of the quantization. For example, multiplying the Franck-Condon shift by a factor 10 only slightly affects the results on the logarithmic scale. Therefore any other source of level broadening like the connections between the crystallites or other phonon coupling will not drastically change the Auger lifetime. For practical use, it also means that a cluster calculation can be an easy way to obtain a rough estimate of the Auger lifetime in bulk silicon. Finally, the use of the bulk silicon dielectric constant in our calculation is not completely justified since it must decrease with the confinement.³¹ A reduction of the dielectric constant leads to a decrease of the Auger lifetime. Therefore our results can be seen as an upper limit for the lifetime.

The high Auger rates confirmed by the above calculation are not, by themselves, exceptional. They are comparable to what can be expected for II-VI or II-V semiconductors. Their importance is in comparison to the other recombination rates in porous silicon which are rather slow. This remark is important, and justifies us to come back to some previous experiment where an Auger

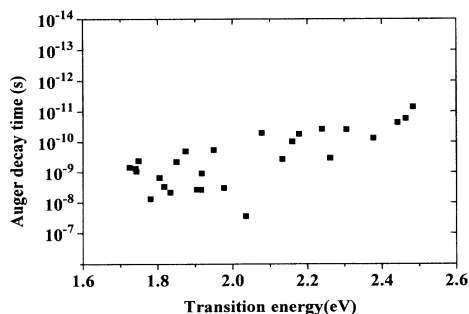


FIG. 11. Calculated lifetime for the Auger recombination in spherical silicon crystallites with respect to the calculated electronic gap. Here the Auger process involves two holes and one electron.

effect can be an alternative explanation to some observations.

C. Revisitation of voltage tunable electroluminescence; importance of the Auger effect

The electroluminescence of *n*-type porous silicon, cathodically polarized in persulfate aqueous solution, can be tuned over a wide range by means of the voltage applied between the substrate and the liquid.³² This has been explained by the selective electroexcitation of the distribution of quantum crystallites by carriers whose energies are determined by the applied voltage. However, the electroluminescence line shape, more precisely its small spectral width, is still unexplained. Here we want to show that the narrow line emission can be seen as a consequence of two competing and simultaneous phenomena: (i) the feeding of a quantum crystallite by selective injection; and (ii) the Auger effect, determined itself, by the selective injection.

Concerning the selective injection, both types of carriers have to be considered. In fact we will emphasize only the majority carriers, since the minority carriers coming from the solvated species have little chance to be in a resonant injection condition. This is justified by the solvation effect, which is known to induce a strong broadening of the energy distribution, and by electrochemical considerations which tend to locate the energy levels of the species far inside the valence band.³³

Under electrical polarization, two classes of crystallites have to be considered.

(i) Crystallites whose electron confinement energy (ΔE) renders possible a carrier injection from the conduction band of the substrate. Their number is proportional to the Fermi-Dirac probability

$$f = \frac{1}{1 + \exp\left[\frac{\Delta E - eV}{kT}\right]}$$

For them, more than one carrier can be injected so they have a very high probability to be submitted to an Auger effect; therefore they become nonluminescent (NL).

(ii) The others in proportion $(1-f)$ remain luminescent. They alone are considered in the following rate equation:

$$\frac{dN^*}{dt} = G(W_r + W_{nr})N,$$

where N^* is the crystallite excited-state population, and G the pumping rate.

The electroluminescence experiments are not performed in the short pulse excitation regime, so the steady-state luminescence intensity I solution of this equation is then

$$I \propto G(1-f). \quad (4)$$

In the photoluminescence quenching experiments, G represents the optical pumping (generally in the UV range); in a first approximation it is not frequency selective. Therefore the luminescence intensity variation fol-

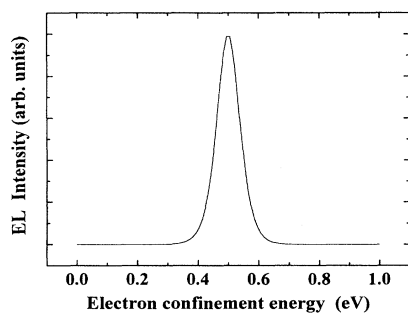


FIG. 12. Room-temperature electroluminescence spectrum calculated from expression (5) for an applied voltage of 0.5 V.

lows $(1-f)$:

$$I \propto 1 - \frac{1}{1 + \exp\left[\frac{\Delta E - eV}{kT}\right]}.$$

This expression well reproduces the steplike behavior shown in Fig. 3. But nothing is new compared to our previous paper (Ref. 8).

Conversely, expression (4), except for electrical pumping, introduces interesting spectral behavior for the electroluminescence. In that case G is not known with accuracy, but we can suppose that it is proportional to the majority-carrier population whose energy matches the crystallite energy levels. In other words, $G \propto f$. Consequently the electroluminescence intensity can be expressed as

$$I \propto f(1-f) =$$

$$I \propto \frac{1}{1 + \exp\left[\frac{\Delta E - eV}{kT}\right]} \left[1 - \frac{1}{1 + \exp\left[\frac{\Delta E - eV}{kT}\right]} \right]. \quad (5)$$

Expression (5) is represented in Fig. 12. As expected, the voltage tunable line-shaped emission well describes the competition between the selective injection and the Auger effect. However, following Ref. 8, to compare this

result to experimental results several additional assumptions have to be made; they concern the potential sharing between electrons and holes. The experimental linewidth is then about twice the calculated linewidth. This can be attributed to a distribution of the potential applied to the crystallite, as has been also invoked in Ref. 8. Nevertheless, this simple model, without any adjustable parameters, where the injection efficiency enters in competition with an excess of injection leading to an efficient Auger effect, gives a simple explanation of the narrow linewidth ($\Delta h\nu \approx 4kT$). It provides an interesting alternative explanation to more complicated models, without requiring knowledge of the energy distribution of minority carriers.

IV. CONCLUSION

This paper gives a description of two nonlinear responses of the photoluminescence of porous silicon. Despite the very different observed phenomena, i.e., voltage-induced photoluminescence quenching and excitation-induced photoluminescence saturation, we have pointed out common features and proposed two different models where carrier injection in confined crystallites plays a major role.

As already observed for bulk silicon,²³ the Auger effect is an efficient nonradiative process which dominates (even at low excitation intensity) as soon as the surfaces are well passivated. On the other hand, porous silicon is known for its naturally good passivation surfaces and for its ability to confine the carriers efficiently. For these reasons we believe that the Auger effect can be the limiting process for charge accumulation; therefore, in the absence of definite proof, it is suspected to be the origin of the photoluminescence saturation.

The Auger effect can also be noticeable when carriers are electrically injected. We believe that this explains the efficient voltage photoluminescence quenching as well as the tunable and spectrally narrow electroluminescence.

For the application point of view, the fast Auger effect can be seen as an efficient switching technique for photoluminescence, as well as for electroluminescence as soon as a fast voltage switching technique becomes available for this porous material. Nevertheless, the efficient Auger effect can also be seen as a major limitation when practical devices need high levels of injection.

¹L. T. Canham, *Appl. Phys. Lett.* **57**, 1046 (1990).

²V. Lehmann and U. Gösele, *Appl. Phys. Lett.* **58**, 856 (1990).

³J. C. Vial, A. Bsiesy, F. Gaspard, R. Hérino, M. Ligeon, F. Muller, R. Romestain, and R. U. Macfarlane, *Phys. Rev. B* **45**, 14 171 (1992).

⁴A. Halimaoui, G. Bomchil, C. Oules, A. Bsiesy, F. Gaspard, R. Hérino, M. Ligeon, and F. Muller, *Appl. Phys. Lett.* **59**, 304 (1991).

⁵A. Bsiesy, F. Muller, I. Mihalcescu, M. Ligeon, F. Gaspard, R. Hérino, R. Romestain, and J. C. Vial, in *Light Emission from Silicon*, edited by J. C. Vial, L. T. Canham, and W. Lang [J. Lumin. **57**, 29 (1993)].

⁶J. C. Vial and I. Mihalcescu, in *Optical Properties of Low Dimensional Silicon Structures*, Vol. 244 of *NATO Advanced Study Institute, Series E: Applied Sciences*, edited by D. Bensahel, L. T. Canham, and S. Ossicini (Kluwer Academic, Boston, 1993), p. 117; L. Tsybeskov, J. V. Vandyshev, and P. Fauchet, *Phys. Rev. B* **49**, 7821 (1994).

⁷J. P. Monchalain, L. Bertrand, G. Rousset, and F. Lepoutre, *J. Appl. Phys.* **56**, 190 (1984).

⁸A. Bsiesy, J. C. Vial, F. Gaspard, R. Hérino, M. Ligeon, I. Mihalcescu, F. Muller, and R. Romestain, *J. Electrochem. Soc.* **141**, 3071 (1994).

⁹M. Koos, I. Pocsik, and E. B. Vazsonyi, *Appl. Phys. Lett.* **62**,

- 1797 (1993).
- ¹⁰F. Trojanek, P. Maly, I. Pelant, A. Hospodkova, V. Kohlova, and J. Valenta, *Thin Solid Films* **255**, 77 (1995).
- ¹¹J. C. Vial, B. Bsiesy, G. Fishman, F. Gaspard, R. Hérino, M. Ligeon, F. Muller, R. Romestain, and R. M. Macfarlane, in *Light Emission from Silicon*, edited by P. M. Fauchet, Y. Aoyagi, and C. C. Tsai, MRS Symposia Proceedings No. 283 (Materials Research Society, Pittsburgh, 1993), pp. 241–246.
- ¹²F. Koch, V. Petrova-Koch, and T. Muschick, in *Light Emission from Silicon* (Ref. 5), p. 271.
- ¹³J. Dziewior and W. Schmid, *Appl. Phys. Lett.* **31**, 346 (1977).
- ¹⁴R. F. Leheny and J. Shah, *Phys. Rev. B* **12**, 3268 (1975).
- ¹⁵R. M. Shelby and R. M. Macfarlane, *Chem. Phys. Lett.* **64**, 545 (1979).
- ¹⁶J. C. Vial, S. Billat, A. Bsiesy, G. Fishman, F. Gaspard, R. Hérino, M. Ligeon, F. Madéore, I. Mihalcescu, F. Muller, and R. Romestain, *Physica B* **185**, 593 (1993).
- ¹⁷R. T. Harley and R. M. Macfarlane, *J. Phys. C* **16**, L1121 (1983).
- ¹⁸R. F. Leheny and C. Lin, *Solid State Commun.* **18**, 1035 (1976).
- ¹⁹T. Suemoto, K. Tanaka, and A. Nakajima, in *Light Emission from Novel Silicon Materials*, edited by Y. Kanemitsu, M. Kondo, and K. Takeda [*J. Phys. Soc. Jpn.* **63**, 190 (1994)].
- ²⁰In this simple model of quantum dots filled with more than one electron-hole pair the Coulomb interaction has been neglected, since carriers are incorporated as a neutral pair.
- ²¹P. J. Dean, R. A. Faulkner, S. Kimura, and M. Ilegems, *Phys. Rev. B* **4**, 1926 (1971).
- ²²W. Schmid, *Phys. Status Solidi B* **84**, 529 (1977).
- ²³E. Yablonovitch and T. Gmitter, *Appl. Phys. Lett.* **49**, 587 (1986).
- ²⁴R. A. Street, *Phys. Rev. B* **23**, 861 (1981).
- ²⁵J. Shah, B. G. Bagley, and F. B. Alexander, Jr., *Solid State Commun.* **36**, 199 (1980).
- ²⁶M. Ghanassi, M. C. Schanne-Klein, F. Hache, A. Ekimov, and D. Ricard, *Appl. Phys. Lett.* **62**, 78 (1992).
- ²⁷Peter T. Landsberg, *Recombination in Semiconductors* (Cambridge University Press, London, 1991).
- ²⁸C. Delerue, G. Allan, and M. Lannoo, *Phys. Rev. B* **48**, 11 024 (1993).
- ²⁹E. Martin, C. Delerue, G. Allan, and M. Lannoo, *Phys. Rev. B* **50**, 18 258 (1994).
- ³⁰J. Bourgoin and M. Lannoo, in *Point Defects in Semiconductors II*, edited by M. Cardona (Springer-Verlag, New York, 1983).
- ³¹R. Tsu and D. Babic, in *Optical Properties of Low Dimensional Silicon Structures* (Ref. 6), p. 203.
- ³²A. Bsiesy, F. Muller, M. Ligeon, F. Gaspard, R. Hérino, R. Romestain, and J. C. Vial, *Phys. Rev. Lett.* **71**, 637 (1993).
- ³³R. Memming, *J. Electrochem. Soc.* **116**, 785 (1969).